

A variational approach to nucleation simulation

Pablo M. Piaggi^{1,3}, Omar Valsson^{2,3}, and Michele Parrinello^{2,3,*}

¹ Theory and Simulation of Materials (THEOS) and National Centre for Computational Design and Discovery of Novel Materials (MARVEL), École Polytechnique Fédérale de Lausanne, CH-1015 Lausanne, Switzerland ²Department of Chemistry and Applied Biosciences, ETH Zurich, c/o USI Campus, Via Giuseppe Buffi 13, CH-6900, Lugano, Switzerland

³Facoltà di Informatica, Istituto di Scienze Computazionali, and National Center for Computational Design and Discovery of Novel Materials (MARVEL), Università della Svizzera italiana (USI), Via Giuseppe Buffi 13, CH-6900, Lugano, Switzerland

*E-mail: parrinello@phys.chem.ethz.ch

Abstract

We study by computer simulation the nucleation of a supersaturated Lennard-Jones vapor into the liquid phase. The large free energy barriers to transition make the time scale of this process impossible to study by ordinary molecular dynamics simulations. Therefore we use a recently developed enhanced sampling method [Valsson and Parrinello, Phys. Rev. Lett. 113, 090601 (2014)] based on the variational determination of a bias potential. We differ from previous applications of this method in that the bias is constructed on the basis of the physical model provided by the classical theory of nucleation. We examine the technical problems associated with this approach. Our results are very satisfactory and will pave the way for calculating the nucleation rates in many systems.

1 Introduction

Nucleation is a process that plays a prominent role in chemistry, engineering and materials science. Among many others, it finds applications in the pharmaceutical industry where crystal shape and structure dramatically affect the drugs potency¹. Moreover, nucleation is not only technologically relevant but also scientifically interesting since it is a paradigmatic example of a self-assembly process². There is thus a great interest in understanding, and eventually controlling, the way in which a new phase emerges from the parent one^{3,4}. In spite of the importance of nucleation, the small scales involved represent a formidable hurdle to experimental studies and thus the details of the process are not easy to unveil. In this regard, molecular simulation and theory could pave the way to a better understanding of the early stages of this process.

One of the simplest examples of homogeneous nucleation is the condensation of a super-saturated vapor. Being a fairly well understood phenomenon, it provides a useful scenario to test new simulation methods. A vapor at a constant temperature and a pressure higher than the vapor pressure is in metastable equilibrium with respect to the liquid phase⁵ and thus it will make a transition to the liquid phase in order to minimize its free energy. However, one of the characteristics of first order phase transitions is the ability to remain in the metastable state due to the existence of a free energy barrier. In this metastable state the system experiences density fluctuations that can be described as the fleeting appearance of small clusters of the new phase. Occasionally the fluctuations are so large that a critical cluster is formed and the whole system condensates. In order for this to occur, the system has to overcome a large energy barrier. This makes nucleation a rare event that cannot be sampled in ordinary simulations. Many solutions to this problem have been proposed⁶⁻⁸ and applications to liquid-vapor nucleation have also been reported⁹⁻¹¹. The closest in spirit to our approach is the work of ten Wolde and Frenkel¹². In this work the free energy landscape of a Lennard-Jones fluid was explored via Monte Carlo

(MC) simulations that used umbrella sampling⁶ to overcome kinetic barriers.

Our paper has a strong methodological connotation since we aim at applying to this well-studied problem the newly developed variationally enhanced sampling (VES) method¹³ in which the bias is determined via a variational procedure based on a suitably defined functional. A few applications of the method have already been presented in the literature^{13–17}. The default way of solving the variational problem is to expand the bias potential in a basis set and use the expansion coefficients as variational parameters. We differ from this approach in that, rather than following this procedure, we use a physically motivated expression derived from classical nucleation theory (CNT). This expression contains two empirical parameters, the supersaturation and the effective surface energy. We shall optimize the functional with respect to these two parameters. This will allow us to understand better the properties of the functional and lay the foundations for future work in which we plan to use a variant of the variational method^{14,18} designed to calculate nucleation rates.

2 Classical nucleation theory

The textbook way of describing nucleation phenomena is CNT. In CNT the cost of forming a cluster of the new phase (in our case the liquid one) can be expressed as:

$$\Delta F^{CNT}(n) = -\Delta\mu n + \sigma n^{2/3}, \quad (1)$$

where n is the number of atoms in the cluster, $\Delta\mu$ is the difference in chemical potential between the two phases (supersaturation), and σ is an effective interfacial energy. The first term represents the energy gain in going into the new more stable phase whereas the second term expresses the energetic cost of forming an interface between the liquid and the vapor. Since on average liquid clusters are spherical, σ can be related to the surface free energy γ by

$\sigma = (36\pi)^{1/3} \rho^{-2/3} \gamma$ where ρ is the density of the new phase. The supersaturation $\Delta\mu$ is often expressed as a dimensionless quantity called supersaturation ratio (S) and defined through $\Delta\mu = k_B T \log S$. The expression in equation (1) differs from the one normally found in textbooks in that the latter uses the drop radius R as a measure of its size. If one makes the assumption that the drops have a spherical shape, the relation between n and R is $n = \frac{4}{3}\pi R^3 \rho$. Substituting this relation in equation (1), the standard expression $\Delta F^{CNT}(R) = -\frac{4}{3}\pi R^3 \rho \Delta\mu + 4\pi R^2 \gamma$ is recovered.

3 Methods

The presence of high barriers often hinders exhaustive sampling in molecular simulations. Enhanced sampling methods aim at solving this problem. Many rely on the introduction of a bias potential V which is a function of a small number of collective coordinates \mathbf{s} . Among these, it is worth noting the historically important umbrella sampling⁶, also used by ten Wolde and Frenkel¹², and metadynamics which has proved to be succesful in a variety of fields^{7,19}. In the next section we describe the theoretical underpinnings of the recently introduced VES¹³.

3.1 Variationally enhanced sampling

As in umbrella sampling and many other enhanced sampling methods, we project the high-dimensional \mathbf{R} space of the N particle system into a much smaller and smoother d -dimensional space by introducing the set of collective variables $\mathbf{s}(\mathbf{R}) = (s_1(\mathbf{R}), s_2(\mathbf{R}), \dots, s_d(\mathbf{R}))$ that give a coarse-grained description of the system. The free energy surface (FES) associated to the CV set \mathbf{s} is defined as:

$$F(\mathbf{s}) = -\frac{1}{\beta} \log \int d\mathbf{R} \delta(\mathbf{s} - \mathbf{s}(\mathbf{R})) e^{-\beta U(\mathbf{R})}, \quad (2)$$

where we have dropped an immaterial constant as we shall also do in the following.

In ref. 13 it was shown how to construct a bias potential $V(\mathbf{s})$ that acts on the CVs via the optimization of the following functional:

$$\Omega[V] = \frac{1}{\beta} \log \frac{\int d\mathbf{s} e^{-\beta[F(\mathbf{s})+V(\mathbf{s})]}}{\int d\mathbf{s} e^{-\beta F(\mathbf{s})}} + \int d\mathbf{s} p(\mathbf{s}) V(\mathbf{s}), \quad (3)$$

where $p(\mathbf{s})$ is a chosen target probability distribution. This functional is convex and it is made stationary by the bias potential:

$$V(\mathbf{s}) = -F(\mathbf{s}) - \frac{1}{\beta} \log p(\mathbf{s}). \quad (4)$$

It follows that once the functional is minimized, the probability distribution of \mathbf{s} in the biased ensemble $p_V(\mathbf{s})$ is equal to the target distribution $p(\mathbf{s})$:

$$p_V(\mathbf{s}) = \frac{e^{-\beta[F(\mathbf{s})+V(\mathbf{s})]}}{\int d\mathbf{s} e^{-\beta[F(\mathbf{s})+V(\mathbf{s})]}} = p(\mathbf{s}). \quad (5)$$

The simplest choice for $p(\mathbf{s})$ is to consider the uniform target distribution $p(\mathbf{s}) = 1/\Omega_s$, where $\Omega_s = \int d\mathbf{s}$ is the volume of CV space. In this case $F(\mathbf{s}) = -V(\mathbf{s})$ as in standard metadynamics. If instead one takes $p(\mathbf{s}) \propto p_0(\mathbf{s})^{1/\gamma}$ where γ is greater than one and $p_0(\mathbf{s})$ is the equilibrium probability distribution of \mathbf{s} in the unbiased ensemble¹⁵, the well-tempered metadynamics distribution is recovered. Other choices have been suggested^{14,16} and here we shall also make use of the added flexibility offered by the freedom of choosing $p(\mathbf{s})$. Once the bias has been determined, a standard reweighting procedure can be used to calculate statistical averages in the unbiased ensemble⁶. Details of the reweighting procedure are provided in the Supplementary Information (SI).

3.2 Collective variable

In order to use the CNT free energy expression to construct the bias, we need to define properly a CV that expresses in analytical and differentiable form the variable n in equation (1) as a function of \mathbf{R} . This requires first defining what is meant by liquid cluster. For this, we follow the procedure suggested by ten Wolde and Frenkel¹². A pair of atoms is considered to belong to the same cluster if their distance is below an assigned radius r_c and each of them has at least n_c neighbors within r_c . Once the clusters have been defined, in order to write a CV that corresponds to the one in CNT one would have had to sort the clusters by their size and consider also their multiplicity, a procedure that would have been expensive and cumbersome.

In their work based on MC, ten Wolde and Frenkel¹² decided to use as CV the largest cluster. The idea behind this choice is that, as the system climbs the barrier, only the largest cluster survives. Eventually the free energy is reweighted to obtain the cluster size distribution (n) as needed in the CNT expression. In the present work, that is based on MD, the use of the largest cluster as CV would have caused problems in the calculation of the forces. In fact, the flag of the largest cluster can change abruptly from one set of atoms to another. Although this could have been remedied, we preferred to use as CV the total number of liquid-like atoms (n_l), a quantity that is easy to calculate. In the SI we describe in detail the calculation of n_l . As we shall see, for small systems where the probability of observing several clusters is negligible, this is a good choice and the resulting free energy as a function of this variable is similar to the CNT expression. For larger systems this is no longer the case but still using a reweighting procedure the cluster size distribution can be obtained (see the SI for details).

3.3 Using the CNT model for the bias potential

Having decided how to represent n , albeit in an approximate form, we first take $p(s)$ to be uniform and write for the bias the functional form:

$$\begin{aligned} V(s; \Delta\mu, \sigma) &= -\Delta F^{CNT}(s; \Delta\mu, \sigma) \\ &= -(-\Delta\mu s + \sigma s^{2/3}), \end{aligned} \quad (6)$$

where $s = n_l$. In equation (6) we have used the fact that if $p(s)$ is uniform, $V(s) = -F(s)$. Expression (6) is then inserted into $\Omega[V]$ and the functional is minimized relative to $\Delta\mu$ and σ . As already discussed in the introduction, this differs from the usual approach in which the bias $V(s)$ is expanded in an orthogonal basis set and the expansion coefficients are used as variational parameters.

In principle at this stage we could have moved to describe the calculation. However, before doing so, a practical issue needs to be addressed. It is in fact convenient to restrict the accessible CV space such that the region in which the system is totally converted into liquid is not explored. This region is not of interest since here we focus on the nucleation barrier and restricting the CV space accelerates the convergence. We shall use $p(s)$ to limit the exploration of the CV space. In particular we shall choose a $p(s)$ that is uniform until a value s_0 and vanishes smoothly beyond it, i.e.:

$$p(s) = \begin{cases} \frac{1}{C} & \text{if } s < s_0 \\ \frac{1}{C} e^{-\frac{1}{2}\beta\kappa(s-s_0)^2} & \text{if } s > s_0 \end{cases}, \quad (7)$$

where s_0 should lie beyond the barrier region, κ is a constant that determines how fast $p(s)$ goes to zero, and C is a normalization constant. The bias potential would be able to produce this $p(s)$ provided that it had sufficient variational flexibility. Since we use instead a bias potential with minimal flexibility, $V(s)$ must be constructed in such a way that it is capable of satisfying

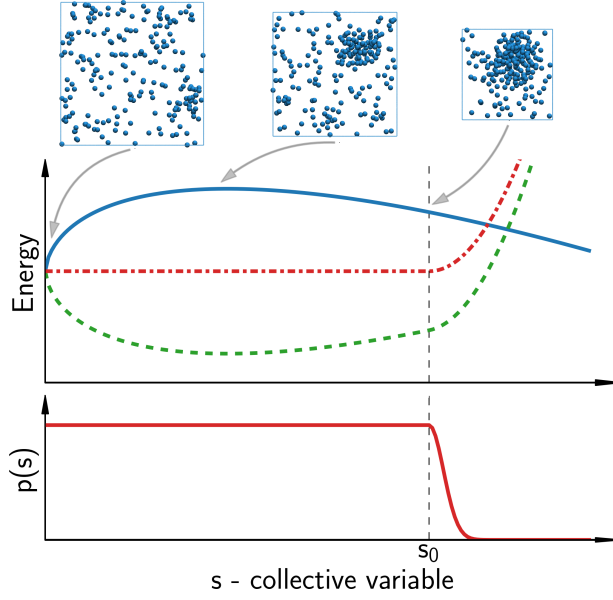


Figure 1: Top plot) One dimensional nucleation free energy surface $F(s)$ (solid blue line), bias potential $V(s)$ (dashed green line), and effective free energy surface $F(s) + V(s)$ (dashed-dotted red line). Bottom plot) Target distribution function $p(s)$ (solid red line). The plots are here for illustrative purposes only and do not reflect the properties of specific physical systems.

equation (4) in all the CV space. A bias potential that is able to do so is:

$$V(s) = \begin{cases} -\Delta F^{CNT}(s; \Delta\mu, \sigma) & \text{if } s < s_0 \\ -\Delta F^{CNT}(s; \Delta\mu, \sigma) + \frac{1}{2}\kappa(s - s_0)^2 & \text{if } s > s_0 \end{cases}. \quad (8)$$

Appropriate values for κ and s_0 can be easily chosen based on a very approximate knowledge of the free energy landscape. In Figure 1 the functional forms of $F(s)$, $V(s)$ and $p(s)$ are depicted.

3.4 Optimization algorithm

Inserting (8) into $\Omega[V]$, the functional becomes a function of $\Delta\mu$ and σ , $\Omega(\Delta\mu, \sigma)$. In order to optimize the functional we need to evaluate the gradient:

$$\begin{aligned}\frac{\partial\Omega(\Delta\mu, \sigma)}{\partial\Delta\mu} &= \langle s \rangle_V - \langle s \rangle_P \\ \frac{\partial\Omega(\Delta\mu, \sigma)}{\partial\sigma} &= -\langle s^{2/3} \rangle_V + \langle s^{2/3} \rangle_P\end{aligned}\quad (9)$$

and the Hessian matrix:

$$H(\Delta\mu, \sigma) = \begin{bmatrix} H_{\Delta\mu\Delta\mu} & H_{\Delta\mu\sigma} \\ H_{\sigma\Delta\mu} & H_{\sigma\sigma} \end{bmatrix} = \beta \cdot \begin{bmatrix} \langle s^2 \rangle_V - \langle s \rangle_V^2 & -\langle s^{5/3} \rangle_V + \langle s \rangle_V \langle s^{2/3} \rangle_V \\ -\langle s^{5/3} \rangle_V + \langle s \rangle_V \langle s^{2/3} \rangle_V & \langle s^{4/3} \rangle_V - \langle s^{2/3} \rangle_V^2 \end{bmatrix}. \quad (10)$$

These expressions involve only expectation values either in the biased ensemble $\langle \rangle_V$ or over the target distribution $\langle \rangle_P$.

Crucial to a succesful optimization is the use of the averaged stochastic gradient descent algorithm²⁰. In the present case this algorithm can be written as an iterative procedure with a fixed step size μ :

$$\begin{aligned}\Delta\mu^{(k+1)} &= \Delta\mu^{(k)} - \mu \left[\frac{\partial\Omega}{\partial\Delta\mu} + H_{\Delta\mu\Delta\mu} \cdot (\Delta\mu^{(k)} - \overline{\Delta\mu}^{(k)}) + H_{\Delta\mu\sigma} \cdot (\sigma^{(k)} - \overline{\sigma}^{(k)}) \right] \\ \sigma^{(k+1)} &= \sigma^{(k)} - \mu \left[\frac{\partial\Omega}{\partial\sigma} + H_{\sigma\Delta\mu} \cdot (\Delta\mu^{(k)} - \overline{\Delta\mu}^{(k)}) + H_{\sigma\sigma} \cdot (\sigma^{(k)} - \overline{\sigma}^{(k)}) \right],\end{aligned}\quad (11)$$

where $\Delta\mu$ and σ are the instantaneous parameters whereas $\overline{\Delta\mu}^{(k)} = k^{-1} \sum_{i=1}^k \Delta\mu^{(i)}$ and $\overline{\sigma}^{(k)} = k^{-1} \sum_{i=1}^k \sigma^{(i)}$ are their averaged counterparts. At each iteration k , both the gradient and the Hessian matrix are estimated in the bias ensemble with a bias potential given by the averaged parameters $\overline{\Delta\mu}^{(k)}$ and $\overline{\sigma}^{(k)}$.

In previous calculations we have used only the diagonal part of the Hessian. Here the use

of the full Hessian is essential for a succesful optimization. In fact the minimization problem is ill-conditioned with a condition number $\sim 10^4$.

Although using the full Hessian allowed us to reach the minimum, we found that a faster convergence could be achieved by making the following change of variables,

$$s(x) = N_0 \left(\frac{x+1}{2} \right)^3, \quad (12)$$

where N_0 is a number slightly larger than the point s_0 where $p(s)$ starts decaying towards zero. This change of variables is akin to the one described in section 2 that transforms the number of atoms n in the droplet into its radius R . Therefore x is related to a characteristic length of the droplet. With this change of variables the new CV is defined in the interval $[-1, 1]$ and, for $s < s_0$, $V(x; \Delta\mu, \sigma)$ can be written as a polynomial:

$$V(x; \Delta\mu, \sigma) = N_0 \Delta\mu \left(\frac{x+1}{2} \right)^3 - N_0^{2/3} \sigma \left(\frac{x+1}{2} \right)^2. \quad (13)$$

It is therefore natural to express $V(x; \Delta\mu, \sigma)$ in terms of Chebyshev polynomials,

$$V(x; \Delta\mu, \sigma) = \sum_{i=0}^3 \alpha_i \cdot T_i(x) \quad (14)$$

where $T_i(x)$ is the Chebyshev polynomial of degree i . Comparison with the expression in equation (13) gives a set of relations between the α_i , and $\Delta\mu$ and σ :

$$\begin{aligned} \alpha_0 &= \frac{5\Delta\mu N_0}{16} - \frac{3\sigma N_0^{2/3}}{8} \\ \alpha_1 &= \frac{15\Delta\mu N_0}{32} - \frac{\sigma N_0^{2/3}}{2} \\ \alpha_2 &= \frac{3\Delta\mu N_0}{16} - \frac{\sigma N_0^{2/3}}{8} \\ \alpha_3 &= \frac{\Delta\mu N_0}{32}. \end{aligned} \quad (15)$$

We can now use, say, α_2 and α_3 as variational parameters, constraining the other two via equations (15). In these new variables, the problem is better behaved and the condition number of the Hessian is reduced to the manageable value of ~ 5 . Although $V(s; \alpha_2, \alpha_3)$ depends only on two variables, the fact that it can be formally expressed as a linear expansion in orthogonal polynomials allows us to use the optimization machinery previously developed to handle this case¹³.

4 Computational details

We have studied condensation from the vapor phase in a Lennard-Jones system in which the interaction potential was truncated and shifted at a cutoff radius $r = 2.5\sigma_{LJ}$, with σ_{LJ} the particle diameter. All MD simulations were performed using LAMMPS²¹ patched with a private development version of the PLUMED 2 enhanced sampling plug-in²². In the following we shall measure all quantities in Lennard-Jones units²³, such that the Lennard-Jones well depth ϵ is the unit of energy and the Lennard-Jones diameter σ_{LJ} is the unit of length. In the definition of the liquid-like atoms we used the values $r_c = 1.5$ and $n_c = 5$ as suggested in ref. 12.

Periodic boundary conditions and a time-step of 0.001 were used in the simulations²³. In all cases the stochastic velocity rescaling thermostat²⁴ and the isotropic version of the Parrinello-Rahman barostat²⁵ were employed. The relaxation time for the thermostat and the barostat were 0.05 and 50, respectively. We employed cubic boxes with different number of particles and a temperature of 0.741 ($T_c = 1.085$). The target pressure of the barostat was set to 0.016. This system setup is similar to that of ref. 12, although the supersaturation is higher in our case.

Each iteration in the optimization of Ω corresponded to 500 MD steps and the step size μ in the optimization was chosen to be 0.001. In all cases 4 multiple walkers were employed, starting half of them in the vapor basin and the rest beyond the nucleation barrier. Due to the

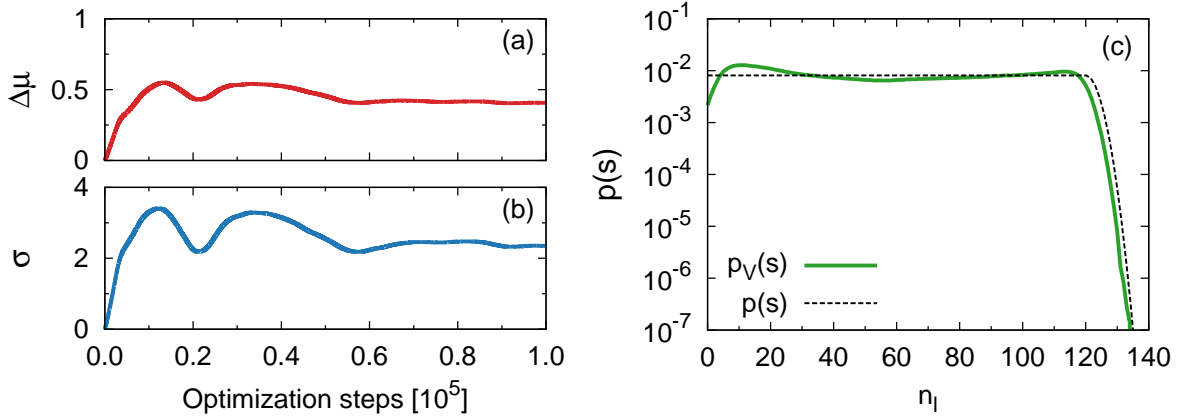


Figure 2: (a)-(b) Evolution of $\Delta\mu$ and σ during the optimization process for a system of 216 particles. (c) Comparison between the sampled probability distribution of the CV n_l $p_V(s)$ and the target probability distribution $p(s)$.

highly non-local nature of the basis sets employed, the use of multiple walkers proved to be instrumental in accelerating the optimization. The initial variational parameters were taken as $\Delta\mu = 0$ and $\sigma = 0$ such that initially the bias was $V(s) = -\frac{1}{\beta} \log p(s)$. The parameters of $p(s)$ were $s_0 = 120$ and $\kappa = 0.1$.

5 Results

As an example of a typical behavior of the optimization process, we show in Figure 2 (a)-(b) the convergence of the variational parameters $\Delta\mu$ and σ as a function of the number of optimization steps in a system with 216 atoms. If we use Lennard-Jones parameters appropriate to argon, the total length of the optimization corresponds to a ~ 100 ns long simulation. A measure of the quality of the variational ansatz in equation (6) is how much the biased distribution $p_V(s)$ differs from the target distribution $p(s)$ (see Figure 2(c)). According to equation (5) these should be identical. Indeed, they are very close but not totally identical. The small discrepancies are a result of the limited variational flexibility of $V(s)$ (equation (6)).

We now turn our attention to the behavior of the free energy as a function of the collective

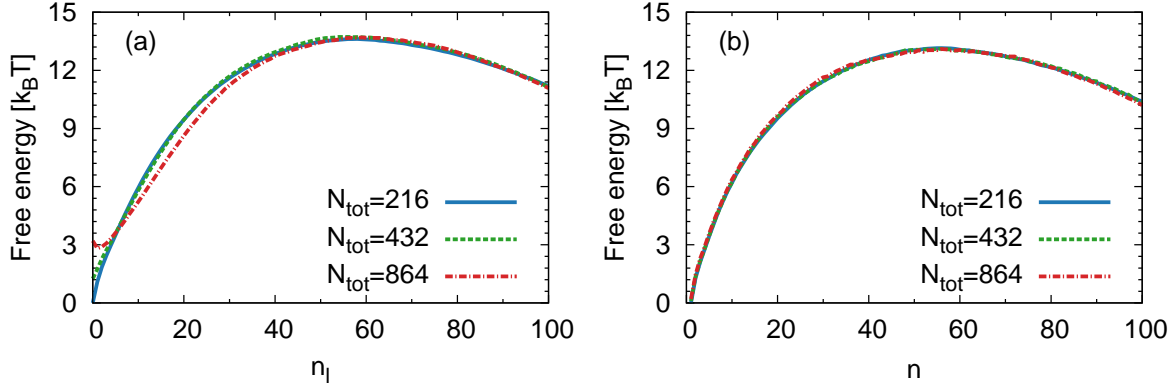


Figure 3: (a) Reweighted free energy as a function of n_l for system sizes $N_{tot} = 216, 432$ and 864 . For small n_l the curves show discrepancies. (b) Reweighted free energy associated to n for the same system sizes as above. All free energies are equal within the statistical error.

variable n_l for three different system sizes (see Figure 3(a)). By and large, the curves are rather similar, however, some differences are observed. This is not surprising since the probability of observing several liquid clusters at one time depends on the system size. This is particularly evident for the low n_l region on which the largest size dependence is observed. This behavior has already been reported for the free energy associated with the size of the largest cluster²⁶. For larger n_l the probability of finding more than one cluster is small, at least for the system sizes studied here, and the size effects are negligible. These finite size effects are quantified in Table 1 where we compare the estimates of $\Delta\mu$ and σ obtained from minimizing Ω to a fit to $F(n_l)$ of the CNT expression. It is seen that the smaller the system, the smaller the deviation of $F(n_l)$ from a CNT-like behavior. However if we reweight our data so as to obtain $F(n)$ (see Figure 3(b)), all the finite size effects disappear. Details of the reweighting procedure and of the calculation of $F(n)$ can be found in the SI. The results can be all fitted to the CNT expression and give what is possibly our best estimate for these parameters (see Table 1), assuming that our data can be described by CNT. The values obtained are consistent with the estimates of $\Delta\mu = 0.530$ and $\sigma = 2.85$ that can be calculated using a coexistence pressure $P_0 = 0.00783$ obtained from Gibbs ensemble simulation¹² and a surface free energy $\gamma = 0.494$ ^{12,27}.

From $F(n)$ we can estimate the nucleus size and the barrier height. The nucleus size n^* at

Table 1: We compare estimations of $\Delta\mu$ and σ for different system sizes. From left to right we show the direct result of the optimization at $5 \cdot 10^5$ steps, a fit of the CNT expression to $F(n_l)$ in the interval $[0, N]$, and a similar fit to $F(n)$ in the interval $[1, N]$. In the last two cases, we show also the error associated to the fit.

System size	Optimization		Fit $F(n_l)$			Fit $F(n)$		
	$\Delta\mu$	σ	$\Delta\mu$	σ	rms error	$\Delta\mu$	σ	rms error
216	0.42(1)	2.4(1)	0.409(6)	2.38(3)	0.39	0.439(2)	2.51(1)	0.12
432	0.41(2)	2.4(3)	0.408(8)	2.37(4)	0.54	0.432(2)	2.48(1)	0.12
864	0.37(4)	2.2(5)	0.38(1)	2.22(7)	0.83	0.436(2)	2.49(1)	0.11

the supersaturation condition studied here corresponds to 56 atoms. We estimated the barrier height defined as $F(n^*) - F(1)$ to be $\sim 13 k_B T$.

In order to test the correctness of the approach described in this work, we have performed a benchmark simulation employing well-tempered metadynamics²⁸. The details of this simulation can be found in the SI. The free energies obtained with the methodology described in this work are equal to those calculated employing well-tempered metadynamics within the statistical error (see Figure S1 in the SI).

6 Discussion and conclusions

We have developed an enhanced sampling method based on the introduction of a bias potential with a physically motivated functional form. In particular, in the context of nucleation, we have employed the functional form of classical nucleation theory for the free energy of formation of a cluster. This idea is put into practice employing a variational principle that allows the estimation of the parameters of the model. In this way the bias potential compensates the underlying free energy of the system.

Our results are encouraging, however they underline the fact that attention must be paid to the choice of the collective variables. In particular for the system of interest here, the choice of n_l as CV has clear computational advantages but it is best applied to small systems where $F(n_l)$ is very close to the free energy associated to the cluster size distribution $F(n)$, that is

system size independent. It must also be noted that for small systems the values for $\Delta\mu$ and σ obtained via the optimization, are very close to those obtained by reweighting the trajectory to get the cluster size distribution and fitting the CNT expression to the results. This might provide an expedite way to estimate the vapor pressure and the surface energy, two quantities of great practical interest.

The lesson learned here will be applied to nucleation rates calculation. In fact, given the results obtained, one could use n_l as the collective variable and employ the approaches suggested either in ref. 18 or ref. 14. Both methodologies rely on introducing a bias potential that leaves the transition region between metastable states untouched. Under this assumption the physical transition time (τ) can be related to the one calculated in a biased simulation (τ_V) by^{18,29,30},

$$\tau = \tau_V \langle e^{\beta V(s,t)} \rangle_V. \quad (16)$$

However, the two methodologies differ from each other in the manner in which the bias potential is constructed. On the one hand, ref. 18 describes a metadynamics based methodology with infrequent deposition of kernels. If the transition is rare but fast then the procedure leads to bias free transition regions therefore fulfilling the assumption that leads to equation (16). On the other hand, the approach described in ref. 14 is based on the construction of a bias potential by means of the variational principle¹³ also used in the present work. This bias potential floods the free energy surface up to a predefined energy level. By construction this approach guarantees bias free transition states and accurate times can be extracted using equation (16). We point out that the independence of $F(n)$ from the system size provides a strong encouragement to limit ourselves to the study of small systems.

Finally, our results provide yet another confirmation of the validity of CNT for liquid-vapor nucleation.

Acknowledgements

P.M.P would like to thank Matteo Salvalaglio and Federico Giberti for useful discussions. The authors acknowledge funding from the National Center for Computational Design and Discovery of Novel Materials MARVEL and the European Union Grant No. ERC-2014-AdG-670227 / VARMET. The computational time for this work was provided by the Swiss National Supercomputing Center (CSCS).

References

- [1] Kwok Chow, Henry H.Y. Tong, Susan Lum, and Albert H.L. Chow. Engineering of pharmaceutical materials: An industrial perspective. *Journal of Pharmaceutical Sciences*, 97(8):2855–2877, 2008.
- [2] William M Jacobs and Daan Frenkel. Self-assembly of structures with addressable complexity. *Journal of the American Chemical Society*, 138(8):2457–2467, 2016.
- [3] Peter G Vekilov. Nucleation. *Crystal growth & design*, 10(12):5007–5019, 2010.
- [4] Roger J Davey, Sven LM Schroeder, and Joop H ter Horst. Nucleation of organic crystals—a molecular perspective. *Angewandte Chemie International Edition*, 52(8):2166–2179, 2013.
- [5] Dimo Kashchiev. *Nucleation: Basic Theory with Applications*. Butterworth-Heinemann, Oxford, 2000.
- [6] Glenn M Torrie and John P Valleau. Nonphysical sampling distributions in monte carlo free-energy estimation: Umbrella sampling. *Journal of Computational Physics*, 23(2):187–199, 1977.

- [7] Alessandro Laio and Michele Parrinello. Escaping free-energy minima. *Proceedings of the National Academy of Sciences*, 99(20):12562–12566, 2002.
- [8] Peter G Bolhuis, David Chandler, Christoph Dellago, and Phillip L Geissler. Transition path sampling: Throwing ropes over rough mountain passes, in the dark. *Annual review of physical chemistry*, 53(1):291–318, 2002.
- [9] Bin Chen, J Ilja Siepmann, Kwang J Oh, and Michael L Klein. Aggregation-volume-bias monte carlo simulations of vapor-liquid nucleation barriers for lennard-jonesium. *The Journal of Chemical Physics*, 115(23):10903–10913, 2001.
- [10] Isamu Kusaka and David W Oxtoby. Identifying physical clusters in vapor phase nucleation. *The Journal of chemical physics*, 110(11):5249–5261, 1999.
- [11] Joonas Merikanto, Hanna Vehkamäki, and Evgeni Zapadinsky. Monte carlo simulations of critical cluster sizes and nucleation rates of water. *The Journal of chemical physics*, 121(2):914–924, 2004.
- [12] Pieter Rein ten Wolde and Daan Frenkel. Computer simulation study of gas–liquid nucleation in a lennard-jones system. *The Journal of Chemical Physics*, 109(22):9901–9918, 1998.
- [13] Omar Valsson and Michele Parrinello. Variational approach to enhanced sampling and free energy calculations. *Physical review letters*, 113(9):090601, 2014.
- [14] James McCarty, Omar Valsson, Pratyush Tiwary, and Michele Parrinello. Variationally optimized free-energy flooding for rate calculation. *Physical review letters*, 115(7):070601, 2015.
- [15] Omar Valsson and Michele Parrinello. Well-tempered variational approach to enhanced sampling. *Journal of chemical theory and computation*, 11(5):1996–2002, 2015.

- [16] Patrick Shaffer, Omar Valsson, and Michele Parrinello. Enhanced, targeted sampling of high-dimensional free-energy landscapes using variationally enhanced sampling, with an application to chignolin. *Proceedings of the National Academy of Sciences*, page 201519712, 2016.
- [17] James McCarty, Omar Valsson, and Michele Parrinello. Bespoke bias for obtaining free energy differences within variationally enhanced sampling. *Journal of Chemical Theory and Computation*, pages 2162–2169, 2016.
- [18] Pratyush Tiwary and Michele Parrinello. From metadynamics to dynamics. *Physical review letters*, 111(23):230602, 2013.
- [19] Omar Valsson, Pratyush Tiwary, and Michele Parrinello. Enhancing important fluctuations: Rare events and metadynamics from a conceptual viewpoint. *Annual Review of Physical Chemistry*, 67(1), 2016.
- [20] Francis Bach and Eric Moulines. Non-strongly-convex smooth stochastic approximation with convergence rate $\mathcal{O}(1/n)$. In *Advances in Neural Information Processing Systems*, pages 773–781, 2013.
- [21] Steve Plimpton. Fast parallel algorithms for short-range molecular dynamics. *Journal of computational physics*, 117(1):1–19, 1995.
- [22] Gareth A Tribello, Massimiliano Bonomi, Davide Branduardi, Carlo Camilloni, and Giovanni Bussi. Plumed 2: New feathers for an old bird. *Computer Physics Communications*, 185(2):604–613, 2014.
- [23] Daan Frenkel and Berend Smit. *Understanding molecular simulation: from algorithms to applications*, volume 1. Academic press, 2001.

- [24] Giovanni Bussi, Davide Donadio, and Michele Parrinello. Canonical sampling through velocity rescaling. *The Journal of chemical physics*, 126(1):014101, 2007.
- [25] Michele Parrinello and Aneesur Rahman. Polymorphic transitions in single crystals: A new molecular dynamics method. *Journal of Applied physics*, 52(12):7182–7190, 1981.
- [26] Lutz Maibaum. Comment on “elucidating the mechanism of nucleation near the gas-liquid spinodal”. *Physical review letters*, 101(1):019601, 2008.
- [27] Cynthia D Holcomb, Paulette Clancy, and John A Zollweg. A critical study of the simulation of the liquid-vapour interface of a lennard-jones fluid. *Molecular Physics*, 78(2):437–459, 1993.
- [28] Alessandro Barducci, Giovanni Bussi, and Michele Parrinello. Well-tempered metadynamics: A smoothly converging and tunable free-energy method. *Physical review letters*, 100(2):020603, 2008.
- [29] Arthur F Voter. Hyperdynamics: Accelerated molecular dynamics of infrequent events. *Physical Review Letters*, 78(20):3908, 1997.
- [30] Helmut Grubmüller. Predicting slow structural transitions in macromolecular systems: Conformational flooding. *Physical Review E*, 52(3):2893, 1995.